Macromolecules

Article

pubs.acs.org/Macromolecules

Follow the Yellow Brick Road: Structural Optimization of Vibrant Yellow-to-Transmissive Electrochromic Conjugated Polymers

Justin A. Kerszulis,[†] Chad M. Amb,[‡] Aubrey L. Dyer,[†] and John R. Reynolds*[,†]

[†]School of Chemistry and Biochemistry, School of Materials Science and Engineering, Center for Organic Photonics and Electronics, Georgia Institute of Technology, Atlanta, Georgia 30332, United States

[‡]The George and Josephine Butler Polymer Laboratories, Department of Chemistry, Center for Macromolecular Science and Engineering, University of Florida, PO Box 117200, Gainesville, Florida 32611, United States

Supporting Information

ABSTRACT: A series of conjugated polymers were designed and synthesized to extract structure−property relationships with the goal of yielding yellow-to-transmissive switching electrochromes. The polymers are based on repeat units of propylenedioxythiophene (ProDOT) in alternation with a variety of arylenes including 1,4-phenylene (ProDOT-Ph), 2,7-fluorene (ProDOT-Fl), 2,7-carbazole (ProDOT-Cbz), 2,5-dimethoxy-1,4-phenylene (ProDOT-Ph(MeO)$_2$), and 2,7-pyrene (ProDOT-Py). Additionally, a random copolymer containing ProDOT and two different arylene units was produced: ProDOT-phenylene-ProDOT-dimethoxyphenylene (R-ProDOT-Ph/Ph(MeO)$_2$) and two polymers with a ProDOT dimer in alternation with pyrene and phenylene composed ProDOT$_2$-pyrene (ProDOT$_2$-Py) and ProDOT$_2$-phenylene (ProDOT$_2$-Ph), respectively. The polymers were synthesized using Suzuki polycondensation. Examinations of the optoelectronic properties via UV−vis−NIR spectroscopy, differential pulse voltammetry, and spectroelectrochemistry show that varying the electron richness of the polymer by utilizing more electron rich arylenes, dimers of ProDOT, or less electron rich arylenes, the oxidation potential could be decreased or increased, respectively, ranging from 270 to 650 mV. Through subtle C−H *ortho* interactions from the arylene unit, yellow neutral state colors were maintained with transmissive or near-transmissive oxidized states. Colorimetry utilizing $L^*a^*b^*$, where a^*b^* values correlate to the chroma or saturation of a color (note: $-a^*$ and $+a^*$ correspond to green and red and $-b^*$ and $+b^*$ correspond to blue and yellow, respectively) and L^* represents the lightness, was used to show the maintenance of yellow colors in the neutral states. Herein, the yellow polymers had L^* values above 84.0, a^* values ranging from −11.6 to 24.8, and b^* values greater than 47.6. In the oxidized states, the most transmissive forms had L^* values above 70.0, a^* values ranging from −2.1 to 2.0, and b^* values ranging from −6.8 to −0.1. These structure−property relationships grant access to conjugated polymers with high energy absorbance in the visible, while allowing variability in redox potentials, providing a deeper understanding in yielding yellow-to-transmissive electrochromic polymers.

INTRODUCTION

The electrochromism of inorganic, organic small molecule, and polymeric based materials has demonstrated the possibility of wide and lucrative applications ranging from displays,[1,2] smart windows,[3,4] E-paper,[5] and E-cloth[6] to dual use emissive/nonemissive systems.[7] Of the materials listed, conjugated polymers hold significant promise as recent advances have demonstrated that they have straightforward synthesis and color tuning,[8−10] coupled with potentially low cost processability.[11,12] The solubility of electrochromic polymers (ECPs) allows for high throughput methods such as spray casting and slot-die coating for large area roll-to-roll processing from aqueous[13] or organic solutions[12] for both display and window applications—necessary for large scale printing and patterning of EC devices.

Our group has focused efforts toward utilizing cathodically coloring polymers that possess vibrantly colored neutral and transmissive oxidized states.[9] Polymers that switch from a colored state to a fully transmissive state are required for applications in window and display technologies where multicolor polymers are not appropriate or desired. Our recent report of the electrochromic polymer ECP-Yellow (herein referred to as ProDOT-Ph for structural comparison with other polymers to be reported) has allowed the completion of a full color palette of solution processable ECPs[9,14] and demonstrated the importance of obtaining a vibrant yellow-to-transmissive electrochrome as this fulfills both of the subtractive primary color sets: cyan−magenta−yellow (CMY) and red−yellow−blue (RYB). Through the use of subtractive color mixing, a wide variety of hues can be obtained for use in full color displays.[15,16] Although our published yellow ECP is the only solution-processable cathodically coloring, yellow-to-transmissive ECP reported to date to our knowledge, it switches at an oxidation potential that is relatively high compared to many of the other electron-rich ECPs we employ. This complicates the use of multiple ECPs on the same

Received: May 23, 2014
Revised: July 21, 2014
Published: August 6, 2014

   dx.doi.org/10.1021/ma501080u | Macromolecules 2014, 47, 5462−5469

Scheme 1. Polymers Synthesized and Examined in This Study

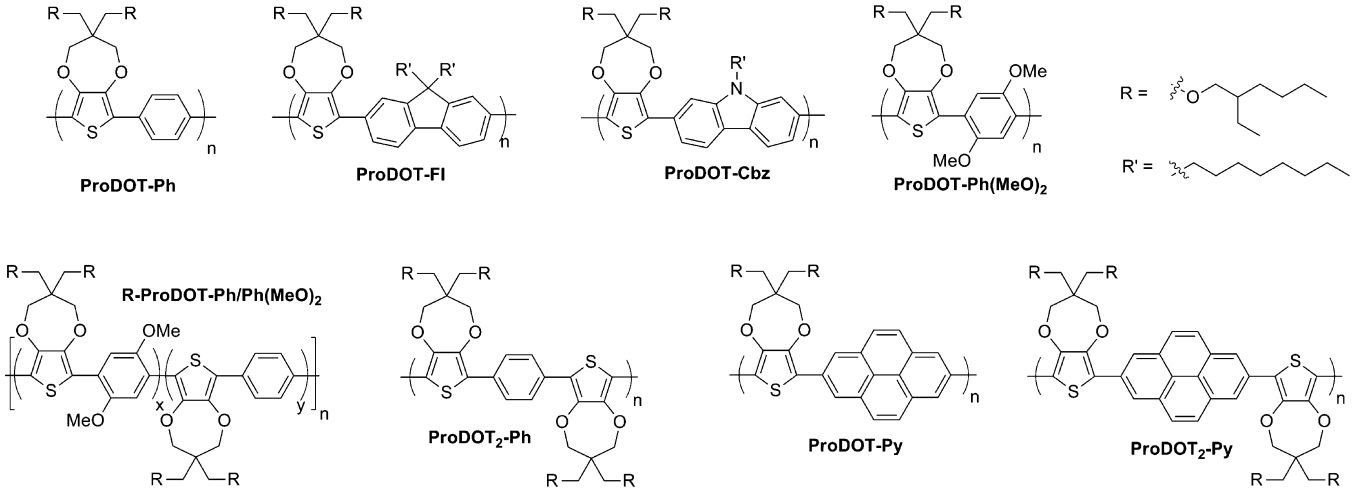

electrode as overoxidation of more easily oxidized polymers can occur when applying the high potential required to switch ProDOT-Ph to the fully transparent state. This observation, along with recent reports of several electrochromic polymers[17−21] and small molecule esters[22−24] that possess yellow states, has motivated a detailed study in developing an understanding of structure−property relationships in a series of ProDOT−arylene conjugated polymers with the aim toward lowering the oxidation potential, allowing a higher level of transparency in the bleached state, while maintaining a vibrant yellow neutral state.

Through varying the choice of an arylene unit in alternation with ProDOT, dimers of ProDOT, or using a random copolymer with ProDOT, we are able to structurally modulate the oxidation potential of seven new ECPs while maintaining yellow or near yellow neutral states that can switch to various transmissive or near transmissive oxidized states. These methods yield insight for the future development of materials with high-energy absorption in the visible region and to vary the electrochemical potentials.

RESULTS AND DISCUSSION

Polymer Synthesis. The repeat unit structures for the polymers synthesized in this effort are shown in Scheme 1. The synthetic details for the preparation of each monomer are given in the Supporting Information (Scheme S1). All of the monomers used were straightforward to produce and are highly scalable from available starting materials. Boronate monomers can generally be produced in high yield using Miyaura borylation or lithium halogen exchange, often with recrystallization as the only purification step. Additionally, recent advances in iridium catalyzed borylation allowed us to access the 2,7-bisborylated pyrene efficiently.[25] Suzuki polycondensation under optimized conditions was chosen as the method to synthesize the polymers as boronic esters are generally environmentally benign.[26]

The Suzuki condensation reactions afforded polymers with molecular weights over 10 kDa (measured by GPC vs polystyrene standards, THF eluent) after initial precipitation into methanol, with the exception of ProDOT-Py and ProDOT$_2$-Py as these polymers were no longer soluble in toluene as the Suzuki reaction progressed. Polymer purification was conducted via Soxhlet extraction with methanol, acetone, and hexane, followed by dissolution with chloroform. ProDOT-Py and ProDOT$_2$-Py were removed from the Soxhlet thimble by washing with near boiling *o*-dichlorobenzene (*o*-DCB). The final polymer solutions were concentrated and stirred at 50 °C for 6 h with 200 mg of diethylammonium diethyldithiocarbamate palladium scavenger[27] dissolved in solution. The solution was then cooled and precipitated into methanol, filtered over a 0.45 μm nylon pad, washed with methanol, collected, and dried under vacuum.

A comparison between the yields and molecular weights (GPC vs polystyrene) is shown in Table 1, and all GPC traces are shown in Figure S1. A majority of the polymers were soluble in THF while ProDOT-Cbz, ProDOT-Py, and ProDOT$_2$-Py required the use of hot 1,3,5-trichlorobenzene (TCB). To be able to make a comparison of the difference in solubility and its effect on molecular weight measurements, GPC of ProDOT-Ph was measured in both solvents and served as a comparison. Attempts using THF for ProDOT-Cbz yielded a chromatogram that was bimodal, and ProDOT-Py and ProDOT$_2$-Py were insoluble in THF and had limited solubility in boiling *o*-DCB as these polymers have a tendency to aggregate, particularly in the case of the pyrenes.[28,29] The polymers in this study have sufficiently high molecular weights to yield saturated conjugation lengths to give the desired spectra and colors, while forming continuous electrode supported films via spray-coating.

Table 1. Comparison of All GPC Estimated Polymer Molecular Weights and Polycondensation Yields

polymer	yield (%)	M_n (kDa)	M_w (kDa)	PDI	solvent
ProDOT-Fl	80	12.0	17.6	1.47	THF
ProDOT-Cbz	95	15.6	45.3	3.00	hot TCB
ProDOT-Ph(MeO)$_2$	38	16.6	24.4	1.46	THF
R-ProDOT-Ph/ Ph(MeO)$_2$	20	14.9	22.4	1.50	THF
ProDOT$_2$-Ph	96	13.8	26.3	1.90	THF
ProDOT-Py	80	8.3	25.0	3.00	hot TCB
ProDOT$_2$-Py	78	9.2	39.1	4.30	hot TCB
ProDOT-Ph	85	20.2	34.4	1.70	THF
		10.8	39.1	2.90	hot TCB

dx.doi.org/10.1021/ma501080u | *Macromolecules* 2014, 47, 5462−5469

A thorough study on the transmetalation step in Suzuki couplings[30,31] allowed us to synthesize ProDOT-Ph(MeO)$_2$ and R-ProDOT-Ph/Ph(MeO)$_2$ with M_n over 10 kDa by changing the base from 3 M K_3PO_4 to 6 M cesium fluoride, though the yields are still significantly lower compared to the other polymerizations—likely due to premature hydrolysis of the boronate ester prior to transmetalation. Initial attempts to attain ProDOT-Ph(MeO)$_2$ and R-ProDOT-Ph/Ph(MeO)$_2$ using potassium phosphate as a base yielded only oligomeric materials. Microwave heating was attempted but yielded products with M_n no higher than 8 kDa.

Redox and Optoelectronic Properties. All of the materials discussed herein have varying band gaps (E_g), absorption maxima (λ_{max}), colorimetric profiles, and oxidation potentials (E_{ox}). To facilitate the comparison of the properties of each polymer, all relevant optical and electrochemical values are provided in Table 2.

Table 2. Optical and Electrochemical Properties of the ECPs Studied

polymer	E_{ox}[a] (mV vs Ag/Ag$^+$)	λ_{max}[b] (nm)	E_g[c] (eV)	λ_{max}[c] (nm)	neutral state L^*, a^*, b^* color coordinates[c]
ProDOT-Ph	500	449	2.42	445	97.4, −8.91, 72.8
ProDOT-Fl	650	436	2.51	435	98.3, −11.6, 58.3
ProDOT-Cbz	450	447[d]	2.48	445	97.0, −10.1, 76.1
		466		472	
ProDOT-Ph(MeO)$_2$	270	423	2.25	480	85.7, 24.8, 60.0
R-ProDOT Ph/Ph(MeO)$_2$	320	439	2.26	462	84.0, 14.5, 59.6
ProDOT$_2$-Ph	300	506	2.23	488	85.6, 31.1, 43.1
ProDOT-Py	460	418[d]	2.59	419	92.0, −9.97, 47.6
		349		350	
ProDOT$_2$-Py	320	476[d]	2.42	480	90.5, −3.43, 70.8
		447		448	
		350		352	

[a]As determined by DPV as the onset of the current for oxidation. [b]For polymer solutions in chlorobenzene. [c]For a film cast onto ITO coated glass. [d]Value taken to establish trend.

Electrochemistry. Differential pulse voltammetry (DPV) was used to determine the effect of each aromatic core coupled with ProDOT (or BiProDOT as is the case of ProDOT$_2$-Ph and ProDOT$_2$-Py) on the E_{ox} of the resulting polymers. All polymers, with the exception of ProDOT-Py and ProDOT$_2$-Py due to solubility issues, were dissolved in 0.5 mg/mL in toluene and drop-cast onto platinum button electrodes and allowed to dry in air. Because of the requirement to dissolve ProDOT-Py and ProDOT$_2$-Py in boiling chlorobenzene or hot *o*-DCB, DPV on button electrodes was not possible as polymer adhesion issues were encountered. To circumvent this, the films were spin-cast onto ITO-coated glass slides using a hot 20 mg/mL solution in *o*-DCB at 2200 rpm for 40 s, achieving transparent films with only minor defects from aggregation. The films on the electrodes were immersed in a solution of 0.2 M lithium bis(trifluoromethyl)sulfonylimide (LiBTI) in propylene carbonate (PC) with a platinum flag counter electrode and a Ag/Ag$^+$ reference electrode (calibrated to Fc/Fc$^+$). All potentials are reported relative to this reference electrode, and further details are provided in the Supporting Information. Because of slow relaxation effects in neutral conjugated polymers from intercalation of solvent and ions,[32−34] films were "broken in" prior to performing DPV by repeated cyclic voltammetry (CV) cycling for 4−6 scans from 0 V to a potential where each polymer film attains its most stable transmissive state. The complete DPV and CV results for all polymers are given in the Supporting Information, Figure S2.

A comparison of the DPV oxidation scans for ProDOT-Ph, ProDOT-Fl, ProDOT-Cbz, and ProDOT$_2$-Ph is shown in Figure 1 where the trend of oxidation potential onsets (from highest to lowest) is as follows: ProDOT-Fl (650 mV) > ProDOT-Ph (500 mV) > ProDOT-Py (460 mV) > ProDOT-Cbz (450 mV) > ProDOT$_2$-Py = R-ProDOT-Ph/Ph(MeO)$_2$ (320 mV) > ProDOT$_2$-Ph (300 mV) > ProDOT-Ph(MeO)$_2$ (270 mV).

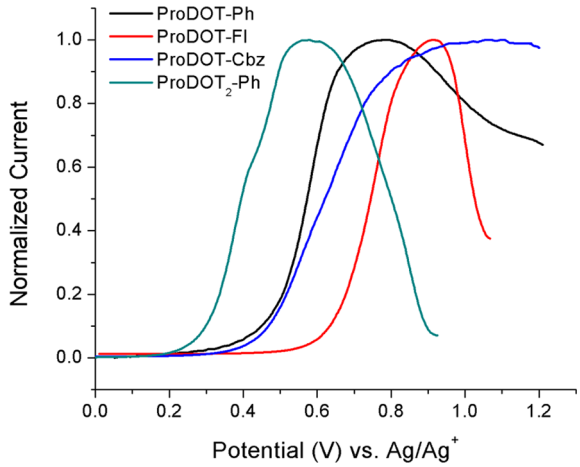

Figure 1. Comparison of E_{ox} acquired via DPV for polymers ProDOT-Ph, ProDOT-Fl, ProDOT-Cbz, and ProDOT$_2$-Ph. Current has been normalized. Reference: 74 mV vs Fc/Fc$^+$.

It can be seen that ProDOT-Fl has the highest E_{ox}, a 150 mV increase compared to ProDOT-Ph. This is attributed to the bridged biphenyl nature of the fluorene, where the additional phenylene ring decreases the HOMO level, giving a higher oxidation potential. ProDOT-Ph has the second highest E_{ox} due to the high aromaticity of the phenylene unit, imparting a low-lying HOMO. The E_{ox} for ProDOT-Py is 190 mV less than ProDOT-Fl and 40 mV less than ProDOT-Ph. For ProDOT-Cbz, the use of carbazole in the repeat unit gave a further decrease in the trend of oxidation potentials and can be attributed to the electron-donating ability of the nitrogen atom bridging the two phenylene rings, raising the HOMO. The random polymer, R-ProDOT-Ph/Ph(MeO)$_2$, and the alternating polymer, ProDOT$_2$-Py, both possess the same E_{ox}. This lowering of potential for R-ProDOT-Ph/Ph(MeO)$_2$ was achieved by randomly incorporating phenylene and electron-rich dimethoxyphenylene into the repeat unit, raising the HOMO relative to ProDOT-Ph. For ProDOT$_2$-Py, the incorporation of an additional electron-rich ProDOT in an alternating repeat unit with pyrene raised the HOMO relative to ProDOT-Py. The E_{ox} of ProDOT$_2$-Ph is the second lowest in the trend by similar reasoning with ProDOT$_2$-Py. The lowest E_{ox} of the series is for ProDOT-Ph(MeO)$_2$, achieved by adding a more electron-rich arylene unit in alternation with a single ProDOT.

All of the polymers discussed have been switched up to 50 cycles with little loss in electroactivity with the exception of ProDOT-Py. Switching for short periods of time was examined (see Chronoabsorptometry section); however, the character-

dx.doi.org/10.1021/ma501080u | Macromolecules 2014, 47, 5462−5469

istics are electrolyte dependent, and optimizing this is beyond of the scope of the paper. Unfortunately, the materials containing pyrene are difficult to dissolve and cast into usable films, and ProDOT-Py exhibits poor switching stability. It should be noted that ProDOT$_2$-Py is a modification of a previously reported yellow ECP where the connectivity of the system is at the 1,6-positions of the pyrene ring, giving it a considerably high E_{ox} value.[20] In our work, the connectivity is through the 2,7-positions of the pyrene ring, affording greater conjugation as evident by the lower oxidation potential of ProDOT$_2$-Py.

Optical Properties. UV/vis spectroscopy of polymer solutions was performed to probe repeat unit structural effects on spectra. The normalized spectra of each solution are shown in Figure 2 with inset photographs of the solutions in vials under white light.

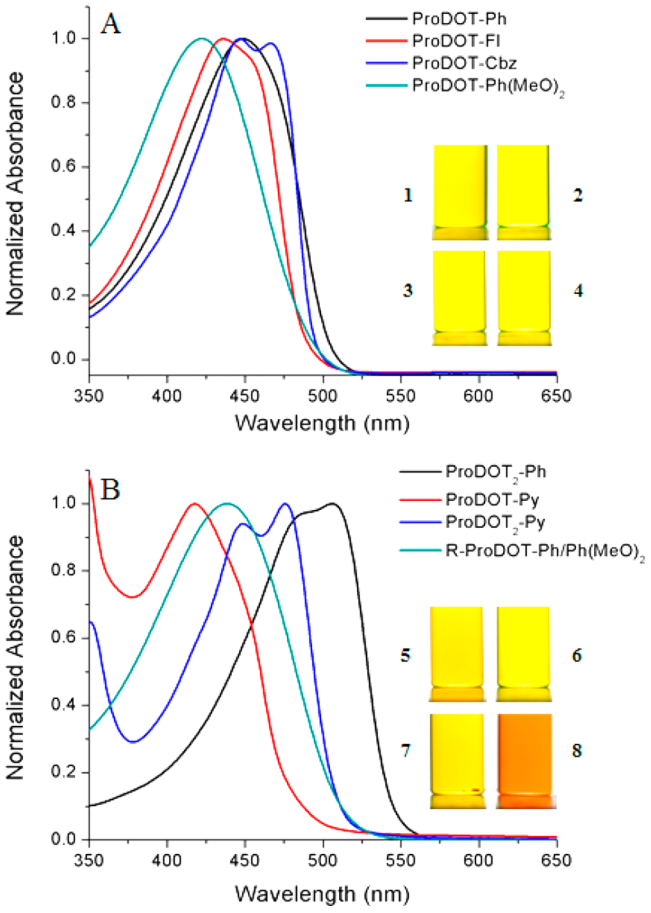

Figure 2. Normalized UV−vis−NIR spectra of polymer solutions in chlorobenzene. Concentrations of solutions for spectra range from 0.05 to 0.02 mg/mL. Photographs of polymer solutions are inset and numbered. (A) ProDOT-Ph (1), ProDOT-Fl (2), ProDOT-Cbz (3), and ProDOT-Ph(MeO)$_2$ (4). (B) R-ProDOT-Ph/Ph(MeO)$_2$ (5), ProDOT-Py (6), ProDOT$_2$-Py (7), and ProDOT$_2$-Ph (8).

When considering the λ_{max} of all polymers in solution (from shortest to longest), the trend is as follows: ProDOT-Py (417 nm) < ProDOT-Ph(MeO)$_2$ (422 nm) < ProDOT-Fl (436 nm) < R-ProDOT-Ph/Ph(MeO)$_2$ (438 nm) < ProDOT-Cbz (446 nm) < ProDOT-Ph (448 nm) < ProDOT$_2$-Py (475 nm) < ProDOT$_2$-Ph (506 nm).

From the trend, ProDOT-Py has the shortest λ_{max}. ProDOT-Ph(MeO)$_2$ has the second shortest λ_{max}, ascribed to the bulky methoxy units in place of the smaller hydrogen atom on the phenylene ring. An alternative possibility for this increase is the raised LUMO from the more electron rich arylene. ProDOT-Fl has the next red-shifted λ_{max}. R-ProDOT-Ph/Ph(MeO)$_2$ has an even longer λ_{max} attributed to backbone relaxation from randomly dispersed phenylene units that possess smaller hydrogen atoms, when compared to ProDOT-Ph(MeO)$_2$. ProDOT-CBz possesses a λ_{max} that is longer than ProDOT-Fl, possibly from electron donation from the nitrogen atom bridging the biphenyl, raising the HOMO. The third longest λ_{max} is for ProDOT-Ph, due to subtle *ortho* C−H interactions from a single phenylene in alternation with ProDOT. The second longest λ_{max} for ProDOT$_2$-Py is believed to be due to the additional ProDOT ring in the repeat allowing S−O interactions between neighboring ProDOTs, facilitating planarity and increasing conjugation along the backbone.[35,36,23] Additionally, increased content of the electron-rich ProDOT unit could serve to raise the HOMO of the polymer. The longest λ_{max} is exhibited by ProDOT$_2$-Ph as per the same reasoning discussed with ProDOT$_2$-Py.

All of the solutions are vibrant shades of yellow except for ProDOT$_2$-Ph, which is a peach color as shown in the inset of Figure 2B. From Figure 2, ProDOT$_2$-Ph has a solution spectral profile similar in shape and width to ProDOT-Cbz and ProDOT-Ph, but red-shifted by ∼60 nm. The peaks at ∼350 nm are typically observed for pyrene related materials.[37,38]

To analyze the absorption profiles at various applied potentials in solid films, all polymers, with the exception of ProDOT-Py and ProDOT$_2$-Py, were dissolved in toluene and spray-cast into films. ProDOT-Py and ProDOT$_2$-Py required spin-coating due to the aforementioned necessity of using hot solutions of *o*-DCB. All of the films were broken in with 4−6 repeated CV cycles, then held at their neutral state potentials, and gradually oxidized in 50 mV steps until oxidized to the most transmissive state. The neutral state spectra of each polymer cast as a film at 0 V can be seen in Figure 3.

In the neutral state, films of polymers exhibited the following trend based on band gap (from highest to lowest): ProDOT-Py (2.59 eV) > ProDOT-Fl (2.51 eV) > ProDOT-Cbz (2.48 eV) > ProDOT-Ph = ProDOT$_2$-Py (2.42 eV) > R-ProDOT-Ph/Ph(MeO)$_2$ (2.26 eV) > ProDOT-Ph(MeO)$_2$ (2.25 eV) > ProDOT$_2$-Ph (2.23 eV).

In the solid state, the trend is comparable to solution, and as expected there is a red-shift in the film absorption profiles. The notable exceptions are polymers that contain dimethoxyphenylene; these exhibit considerable red-shifted spectra in the solid state relative to their solution forms. Random copolymer R-ProDOT-Ph/Ph(MeO)$_2$ has the third lowest E_g, indicating that there is an increase in conjugation along the backbone, facilitated by the methoxy groups on the phenylene cores inducing S−O interactions with their ProDOT neighbors. The second lowest E_g is for ProDOT-Ph(MeO)$_2$, slightly lower than R-ProDOT-Ph/Ph(MeO)$_2$—little change in the E_g. However, due to dimethoxy-substituted phenylene replacing unsubstituted phenylene, ProDOT-Ph(MeO)$_2$ has a narrower absorption profile, lacking high-energy transitions imparted by phenylene neighbors that would induce strain in the backbone. ProDOT$_2$-Ph exhibits an absorption profile of similar shape to that of ProDOT-Ph but is red-shifted by ∼40 nm, giving it a vibrant peach color.

Spectroelectrochemistry. All polymer films were steadily oxidized from their neutral forms to the most transmissive, oxidized state in 50 mV steps. Of the series, ProDOT-Cbz

dx.doi.org/10.1021/ma501080u | *Macromolecules* 2014, 47, 5462−5469

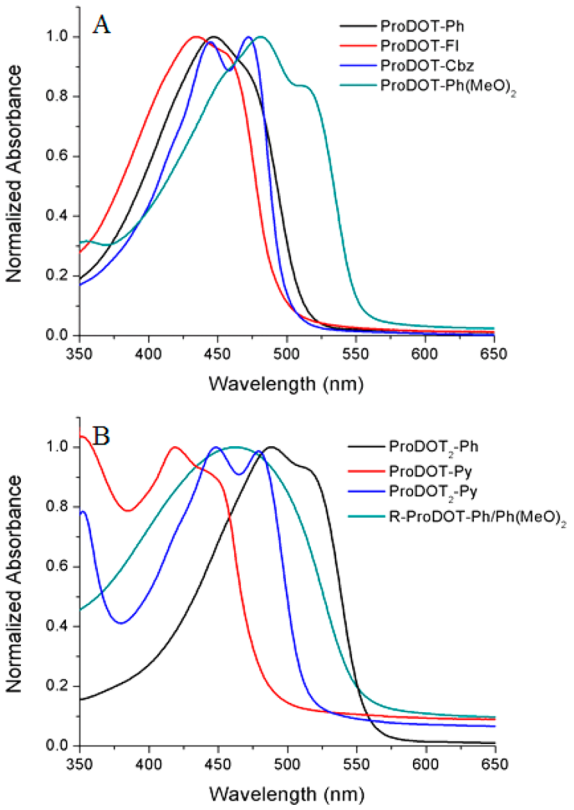

Figure 3. Normalized neutral state spectra of cast polymer films on ITO-coated glass in 0.2 M LiBTI/PC electrolyte solution: (A) ProDOT-Ph, ProDOT-Fl, ProDOT-Cbz, and ProDOT-Ph(MeO)$_2$; (B) R-ProDOT-Ph/Ph(MeO)$_2$, ProDOT-Py, ProDOT$_2$-Py, and ProDOT$_2$-Ph.

exhibited the purest yellow neutral state and switched to the most transmissive oxidized state and is exemplified by the spectroelectrochemical series and photographs shown in the inset to Figure 4 where the peak at 610 nm is assigned to a polaron and the broad absorption into the NIR is attributed to a bipolaron.[39] Upon oxidation to 1100 mV ProDOT-Cbz is able to achieve the most transmissive oxidized state, and the

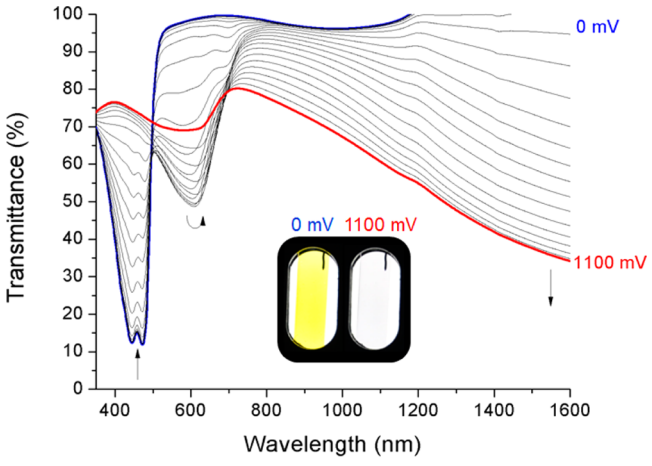

Figure 4. UV−vis/NIR transmittance spectroelectrochemistry of ProDOT-Cbz film spray-cast from a ∼2 mg/mL solution of toluene. Electrochemical oxidation was carried out in a 0.2 M LiBTI/PC electrolyte solution. The applied potential was increased in 50 mV steps from 0 to 1100 mV.

neutral state color is closer to yellow as defined by Munsell (L^* = 81.7, a^* = 4.0, b^* = 79.8)[40] than the other polymers. At ∼1180 nm, the transmittance is greater than 100% in the neutral state. This is due to index matching between the electrolyte, polymer layer, ITO, and glass exhibiting behavior akin to an antireflective coating, allowing more light to pass through the film and reach the detector relative to the baseline.[41,42] The spectroelectrochemistry for all others are provided in Figure S3.

A comparison of ProDOT-Cbz, R-ProDOT-Ph/Ph(MeO)$_2$, and ProDOT-Ph in the neutral and most oxidized transmissive states is shown in Figure 5. These three polymers were chosen

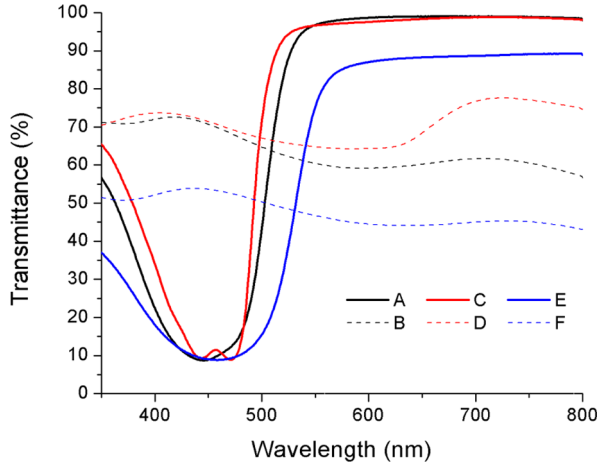

Figure 5. Comparison between the transmittance (%) of the neutral and oxidized forms of ProDOT-Ph, ProDOT-Cbz and R-ProDOT-Ph/Ph(MeO)$_2$. Films were sprayed to an absorbance of ∼1.0 au. (A) ProDOT-Ph at 0 mV, (B) ProDOT-Ph at 1150 mV, (C) ProDOT-Cbz at 0 mV, (D) ProDOT-Cbz at 1100 mV, (E) R-ProDOT-Ph/Ph(MeO)$_2$ at 0 mV, and (F) R-ProDOT-Ph/Ph(MeO)$_2$ at 950 mV.

as they display a true yellow color as defined by Munsell while also achieving the highest transmission in the oxidized state of the family reported. Of the three polymers one can see that ProDOT-Cbz is able to acquire the most transmissive oxidized state (also evident in the photographs in Figure S5) and is the most transmissive of all of the polymers studied. This is possible due to lower absorption of residual long wavelength visible light with an oxidation potential that is 50 mV less than ProDOT-Ph.

Chronoabsorptometry. To understand the rate at which the bleaching/coloring processes occur under repeated cycles between the fully colored and bleached states, chronoabsorptometry was performed. The polymer films, cast onto ITO/glass, were immersed in a fresh electrolyte solution, broken in with 4−6 CV cycles, and then switched using potential square-waves between the extreme states in intervals of 10 to 1/4 s, while the transmission was measured at a single wavelength (polymer λ_{max} determined from spectroelectrochemistry).

Chronoabsorptometry of ProDOT-Cbz is shown in Figure 6 with results for the other materials in Figure S4. At 1 s and longer intervals ProDOT-Cbz possessed a change in transmittance ($\Delta\%T$) of 51%, switching from a vibrant yellow neutral state to a highly transmissive oxidized state. At shorter switching intervals, $\Delta\%T$ for this polymer decreased significantly to 40% at 1/2 s and 30% at 1/4 s, both switching from vibrant yellow states to blue/gray intermediate states.

dx.doi.org/10.1021/ma501080u | Macromolecules 2014, 47, 5462−5469

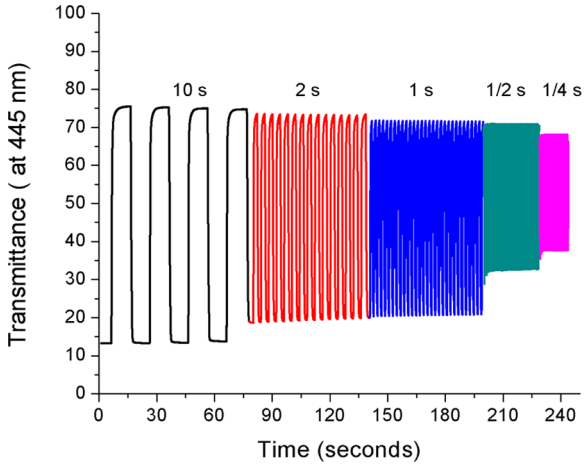

Figure 6. Chronoabsorptometry of ProDOT-Cbz measured at 445 nm from 0 to 1100 mV in an electrolyte solution.

Colorimetry and Photographs. To elucidate the color properties of each polymer, colorimetry within the switching window was measured, and photographs were obtained for each system. The color of each polymer film was assessed by utilizing the CIE 1976 $L^*a^*b^*$ Color Space with a D50 illuminant as detailed in the Supporting Information. The colorimetry of ProDOT-Cbz is shown in Figure 7 and Figure

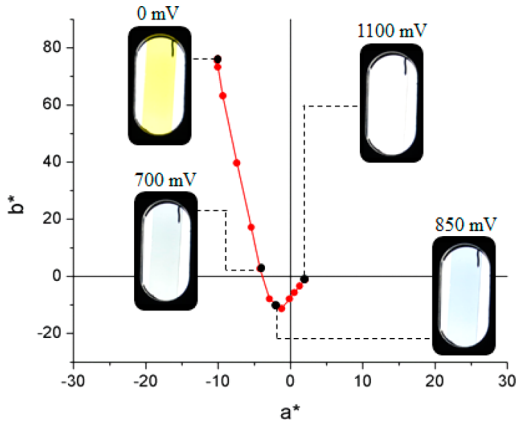

Figure 7. Colorimetry a^*b^* (CIE 1976 $L^*a^*b^*$ Color Space) color coordinates of a thin film of ProDOT-Cbz taken as a function of level of electrochemical oxidation (0–1100 mV, 50 mV steps). The film shown possesses an optical density of 0.8 au at 445 nm.

S5. Over a range of film thicknesses (measured by optical density), from thin films with low optical density (0.65 absorbance) to thick films with higher optical density (1.42 absorbance), a^*b^* color values progress further from the origin, increasing color saturation. Values of a^* minimally change from −7.7 to −10.6 while b^* values progress from 60 and to 100, giving more saturated yellow colors with increasing thickness. The polymer exhibits two transmissive oxidized states. The first at 700 mV is transmissive and color neutral as seen in the photographs; however, at this voltage the transmission is 50% hence, color neutral with low a^*b^* values. At 850 mV, the polymer exhibits a blue intermediate state due to residual absorption peaking at 610 nm as can be seen in Figures 4 and 7. The most transparent state is achieved at a voltage of 1100 mV; the final voltage before overoxidation occurs. The polymer is capable of solid state emission as supported by fluorescence studies, and photographs of solid films under UV exposure are provided in the Supporting Information Figures S7–S9. All of these materials possess various neutral state shades of yellow and exhibit transmissive or near-transmissive oxidized states as can be seen in the Supporting Information, Figure S5.

The lightness (L^*) of all the polymers during electrochromic switching begin at relatively high L^* in their neutral forms with values greater than 84. To aid in the comparison between the neutral and oxidized state, L^* of all materials have been provided in the Supporting Information (Figure S6). Upon oxidation to the most transmissive forms, the polymers possess L^* values of no less than 84 with the exceptions of R-ProDOT-Ph/Ph(MeO)$_2$, ProDOT-Py, and ProDOT$_2$-Py due to residual absorption of visible light in the most oxidized state.

For yellow ECPs undergoing redox processes, the subtle change in L^* is related to the sensitivity of the $\bar{y}(\lambda)$ component of the CIE standard observer color matching functions ($\bar{y}$ peaks at 555 nm), and these functions are used when calculating Y according to CIE for the calculation of L^*.[43] As illustrated in Figure 8, the spectral sensitivity curve of this standard observer

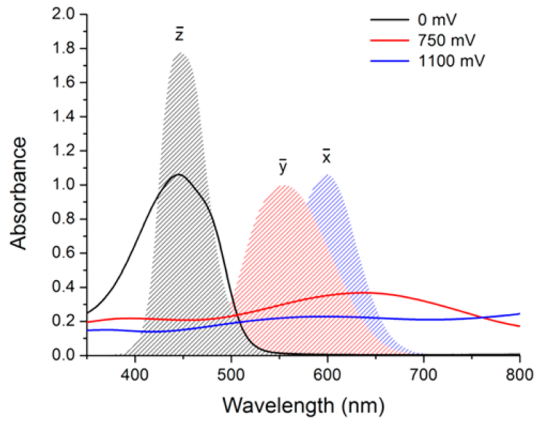

Figure 8. Absorption spectra of ProDOT-Ph in the neutral (0 mV), intermediate (750 mV), and fully oxidized (1100 mV) states. CIE standard observers $\bar{x}$, $\bar{y}$, and $\bar{z}$ are overlaid.

has little overlap with the neutral state absorption spectra of ProDOT-Ph (or any of the polymers discussed herein). Once oxidized to the intermediate state, ProDOT-Ph (and the other yellow ECPs) exhibits a significant dip in lightness as the absorption spectra of these states now overlap with the $\bar{y}(\lambda)$ component.

To gain a greater understanding of the breadth of colors achieved in the neutral state, we present a colorimetric comparison of all polymers studied. As shown in Figure 9, all neutral state colors range from vibrant yellows similar to ProDOT-Ph (ProDOT-Cbz possessing nearly the same a^*b^* values during switching) to colors bordering on or falling into the orange region of the $L^*a^*b^*$ color space such as the case for ProDOT$_2$-Ph.

Films of ProDOT-Ph, ProDOT-Cbz, and R-ProDOT-Ph/Ph(MeO)$_2$ in the neutral, intermediate, and fully oxidized states on one piece of ITO-coated glass in electrolyte solution are shown in Figure 10. Aesthetically speaking, all three polymers appear yellow to the eye with low a^* and high b^* values describing them as yellow hues. Of the three, R-ProDOT-Ph/Ph(MeO)$_2$ has the lowest oxidation potential (320 mV) with a similar yellow neutral state. Unfortunately, it suffers from residual color in its most oxidized form.

dx.doi.org/10.1021/ma501080u | Macromolecules 2014, 47, 5462–5469

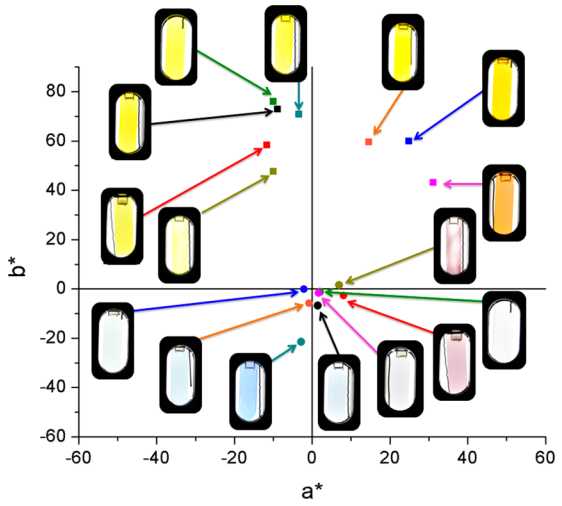

Figure 9. Colorimetry of all polymers with initial neutral state optical density of ∼0.8 with the exception of ProDOT-Py and ProDOT$_2$-Py (optical density of ∼1.0). Squares represent neutral states, and circles represent the most oxidized states. ProDOT-Ph (black), ProDOT-Fl (red), ProDOT-Cbz (green), ProDOT-Ph(MeO)$_2$ (blue), R-ProDOT-Ph/Ph(MeO)$_2$ (orange), ProDOT$_2$-Ph (pink), ProDOT-Py (brown), and ProDOT$_2$-Py (dark cyan).

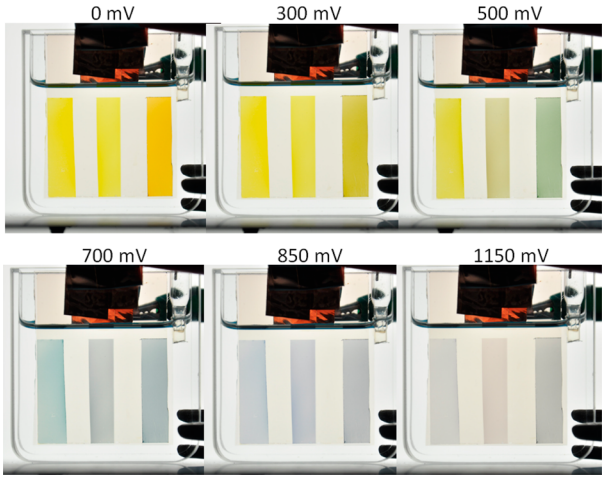

Figure 10. Photographic comparison between ProDOT-Ph (left), ProDOT-Cbz (middle), and R-ProDOT-Ph/Ph(MeO)$_2$ (right). All three polymers were spray cast using a mask (∼1 au) onto a single pane of ITO-coated glass using a clean pane of ITO-coated glass of equal size as a counter electrode.

CONCLUSION

We have successfully synthesized seven new electrochromic polymers via Suzuki polycondensation conditions. All of the materials maintained yellow and near-yellow neutral states while varying the oxidation potential. They all possess oxidation potentials that increase in the order of ProDOT-Ph(MeO)$_2$ < ProDOT$_2$-Ph < ProDOT$_2$-Py = R-ProDOT-Ph/Ph(MeO)$_2$ < ProDOT-Cbz < ProDOT-Py < ProDOT-Ph < ProDOT-Fl. Of the family, ProDOT-Cbz shows optical properties well suited for yellow-to-transmissive switching applications and also has a decreased oxidation potential with respect to ProDOT-Ph, our original yellow electrochromic polymer.

In general, phenylene-type rings neighboring ProDOTs in a polymer chain lead to absorption of high-energy light in the visible, yielding vibrant yellow neutral states. These rings are highly aromatic and cause the polymers to oxidize at elevated potentials. However, the addition of electron-donating oxygen atoms on phenylene rings or the introduction of additional ProDOT units can decrease oxidation potentials. The decrease in oxidation potential comes at the cost of red-shifting or broadening of the overall spectrum, thus yielding orange hues, and is a challenge that will need to be addressed in the development of future yellow systems.

ASSOCIATED CONTENT

Supporting Information

All electrochemical and colorimetry details, photography settings, synthetic procedures, GPC analysis, optical and electrochemical characterizations, and ^{1}H NMR spectra of all polymers. This material is available free of charge via the Internet at http://pubs.acs.org.

AUTHOR INFORMATION

Corresponding Author

*E-mail reynolds@chemistry.gatech.edu (J.R.R.).

Notes

The authors declare no competing financial interest.

ACKNOWLEDGMENTS

We thank BASF for financial support along with Mike Craig and Ray Bulloch for synthetic and technical support, respectively. We thank the Max-Planck Institute for Polymer Research and Wojciech (Wojtek) Pisula and Xin Guo for GPC studies performed with TCB.

REFERENCES

(1) Möller, M.; Leyland, N.; Copeland, G.; Cassidy, M. *Eur. Phys. J. Appl. Phys.* **2010**, *51* (3), 33205−33208.
(2) Corr, D.; Bach, U.; Fay, D.; Kinsella, M.; McAtamney, C.; O'Reilly, F.; Rao, S. N.; Stobie, N. *Solid State Ionics* **2003**, *165*, 315−321.
(3) Baetens, R.; Jelle, B. P.; Gustavsen, A. *Sol. Energy Mater. Sol. Cells* **2010**, *94* (2), 87−105.
(4) Barratt, J.; Dowd, K. *Des. Manage. Rev.* **2006**, *17* (4), 25−30.
(5) Liu, H.; Crooks, R. M. *Anal. Chem.* **2012**, *84* (5), 2528−2532.
(6) Ding, Y.; Invernale, M. A.; Sotzing, G. A. *ACS Appl. Mater. Interfaces* **2010**, *2* (6), 1588−1593.
(7) Puodziukynaite, E.; Oberst, J. L.; Dyer, A. L.; Reynolds, J. R. *J. Am. Chem. Soc.* **2012**, *134* (2), 968−978.
(8) Gunbas, G.; Toppare, L. *Chem. Commun.* **2012**, *48* (8), 1083−1101.
(9) Dyer, A. L.; Thompson, E. J.; Reynolds, J. R. *ACS Appl. Mater. Interfaces* **2011**, *3* (6), 1787−1795.
(10) Amb, C. M.; Dyer, A. L.; Reynolds, J. R. *Chem. Mater.* **2011**, *23* (3), 397−415.
(11) Søndergaard, R. R.; Hösel, M.; Krebs, F. C. *J. Polym. Sci., Part B: Polym. Phys.* **2013**, *51* (1), 16−34.
(12) Jensen, J.; Dam, H. F.; Reynolds, J. R.; Dyer, A. L.; Krebs, F. C. *J. Polym. Sci., Part B: Polym. Phys.* **2012**, *50* (8), 536−545.
(13) Shi, P.; Amb, C. M.; Dyer, A. L.; Reynolds, J. R. *ACS Appl. Mater. Interfaces* **2012**, *4* (12), 6512−6521.
(14) Amb, C. M.; Kerszulis, J. A.; Thompson, E. J.; Dyer, A. L.; Reynolds, J. R. *Polym. Chem.* **2011**, *2* (4), 812−814.
(15) Bulloch, R. H.; Kerszulis, J. A.; Dyer, A. L.; Reynolds, J. R. *ACS Appl. Mater. Interfaces* **2014**, *6* (9), 6623−6630.
(16) Watanabe, Y.; Nagashima, T.; Nakamura, K.; Kobayashi, N. *Sol. Energy Mater. Sol. Cells* **2012**, *104*, 140−145.
(17) Oguzhan, E.; Bilgili, H.; Koyuncu, F. B.; Ozdemir, E.; Koyuncu, S. *Polymer* **2013**, *54* (23), 6283−6292.

(18) Xu, C.; Zhao, J.; Yu, J.; Cui, C. *Electrochim. Acta* **2013**, *96*, 82−89.
(19) Dey, T.; Invernale, M. A.; Ding, Y.; Buyukmumcu, Z.; Sotzing, G. A. *Macromolecules* **2011**, *44* (8), 2415−2417.
(20) İçli-Özkut, M.; Öztaş, Z.; Algi, F.; Cihaner, A. *Org. Electron.* **2011**, *12* (9), 1505−1511.
(21) Liou, G. S.; Lin, H. Y. *Macromolecules* **2009**, *42* (1), 125−134.
(22) Imaizumi, K.; Watanabe, Y.; Nakamura, K.; Omatsu, T.; Kobayashi, N. *Phys. Chem. Chem. Phys.* **2011**, *13* (25), 11838−11840.
(23) Nielsen, C. B.; Angerhofer, A.; Abboud, K. A.; Reynolds, J. R. *J. Am. Chem. Soc.* **2008**, *130* (30), 9734−9746.
(24) Urano, H.; Sunohara, S.; Ohtomo, H.; Kobayashi, N. *J. Mater. Chem.* **2004**, *14*, 2366−2368.
(25) Coventry, D. N.; Batsanov, A. S.; Goeta, A. E.; Howard, J. A. K.; Marder, T. B.; Perutz, R. N. *Chem. Commun.* **2005**, 2172−2174.
(26) Murage, J.; Eddy, J. W.; Zimbalist, J. R.; McIntyre, T. B.; Wagner, Z. R.; Goodson, F. E. *Macromolecules* **2008**, *41* (20), 7330−7338.
(27) Nielsen, K. T.; Bechgaard, K.; Krebs, F. C. *Macromolecules* **2005**, *38* (3), 658−659.
(28) Simona, F.; Nussbaumer, A. L.; Haner, R.; Cascella, M. *J. Phys. Chem. B* **2013**, *117* (8), 2576−2585.
(29) Podeszwa, R.; Szalewicz, K. *Phys. Chem. Chem. Phys.* **2008**, *10* (19), 2735−2746.
(30) Amatore, C.; Jutand, A.; Le Duc, G. *Chem.—Eur. J.* **2011**, *17* (8), 2492−2503.
(31) Amatore, C.; Jutand, A.; Le Duc, G. *Angew. Chem., Int. Ed.* **2012**, *51* (6), 1379−1382.
(32) Inzelt, G. *Chem. Biochem. Eng. Q.* **2007**, *21* (1), 1−14.
(33) Odin, C.; Nechtschein, M.; Hapiot, P. *Synth. Met.* **1992**, *47* (3), 329−350.
(34) Odin, C.; Nechtschein, M. *Synth. Met.* **1991**, *44* (2), 177−188.
(35) Lin, C.; Endo, T.; Takase, M.; Iyoda, M.; Nishinaga, T. *J. Am. Chem. Soc.* **2011**, *133* (29), 11339−11350.
(36) Spencer, H. J.; Skabara, P. J.; Giles, M.; McCulloch, I.; Coles, S. J.; Hursthouse, M. B. *J. Mater. Chem.* **2005**, *15* (45), 4783−4792.
(37) Lu, G.; Shi, G. *J. Electroanal. Chem.* **2006**, *586* (2), 154−160.
(38) Tang, C.; Liu, F.; Xia, Y. J.; Xie, L. H.; Wei, A.; Li, S. B.; Fan, Q. L.; Huang, W. *J. Mater. Chem.* **2006**, *16* (41), 4074−4080.
(39) Hwang, J.; Schwendeman, I.; Ihas, B. C.; Clark, R. J.; Cornick, M.; Nikolou, M.; Argun, A.; Reynolds, J. R.; Tanner, D. B. *Phys. Rev. B* **2011**, *83* (19), 195121.
(40) Berns, R. S. In *Billmeyer and Saltzman's Principles of Color Technology*, 3rd ed.; John Wiley & Sons: New York, 2000.
(41) Kaihovirta, N.; Larsen, C.; Edman, L. *ACS Appl. Mater. Interfaces* **2014**, *6* (4), 2940−2947.
(42) Bhuvana, T.; Kim, B.; Yang, X.; Shin, H.; Kim, E. *Angew. Chem., Int. Ed.* **2013**, *52* (4), 1180−1184.
(43) Wyszecki, G. S.; Stiles, W. S. In *Color Science: Concepts and Methods, Quantitative Data and Formulae*, 2nd ed.; Wiley-Interscience: New York, 2000.